Lasing Mechanism of ZnO Nanowires/Nanobelts at Room Temperature

Bingsuo Zou,*,†,‡ RuiBin Liu,†,‡ Feifei Wang,†,‡ Anlian Pan,†,‡ Li Cao,†,‡ and Zhong L. Wang§

Micro-Nano Technologies Research Center Hunan University, Changsha, 410082, China; Beijing National Lab for Condensed Matter Physics, Institute of Physics, CAS, Beijing 100080, China; School of Materials Science and Engineering, Georgia Institute of Technology, Atlanta, Georgia 30332-0245

Received: March 4, 2006; In Final Form: April 28, 2006

ZnO has become the focus of photonics and optoelectronic research. We prepared pure Mn(II) doped ZnO nanowires with a controlled reduction reaction by carbon in an asymmetrical tube. Careful time-resolved photoluminescence experimental study indicates three types of lasing mechanisms: exciton−exciton interaction, bipolaronic exciton condensation, and plasma; these exist in different ZnO nanowires, which can be changed by doping Mn in ZnO nanowire. The transformation between varied mechanisms is discussed in detail with their spectral behaviors. These results are important in the design of future violet−blue luminescence and display devices.

1. Introduction

Zinc oxide, a wide band-gap semiconductor (3.37 eV) at room temperature, is attracting much interest recently due to its optical and electric properties. The wide direct band gap and large exciton binding energy of 60 meV predict its potential as violet light emitting devices at room temperature and even higher.[1] Optically pumped lasing behaviors have been widely studied for single crystals, expitaxial and polycrystalline thin film, and powder of ZnO,[2−5] and both the exciton−exciton collision and random scattering mechanisms have been proposed.[6,7] ZnO nanostructures has been demonstrated to exhibit stimulated emission at room temperature,[8] and room-temperature ultraviolet lasing is contributed by the Fabry−Pyrot effect.[9] Later observation of waveguide in ZnO nanowires[10] indicates a long coupling length between excitons and/or light, which may lead to new lasing mechanisms like polariton. A variety of nanostructures synthesized by Wang et al.[11] have greatly expanded the family of ZnO, which are ideal for studying novel exciton behavior in various shaped nanostructures.

In this paper, zinc oxide nanowires were prepared with a simple reduction reaction method in a tube furnace. All samples were examined by the ICP technique to determine their composition. Steady He−Cd laser, fs pulsed Ti:sapphire laser systems were used to pump the nanowires dispersed on a quartz substrate or dispersed in ethanol. Their emission spectra were detected by the photomultiplier attached by the spectrometer and streak camera. The spectrometer resolution is 0.1 nm, and the streak camera has resolution of 20ps.

2. Growth of Pure ZnO Nanobelts.

The ZnO nanobelts were grown by a vapor−solid process.[11] ZnO powder and graphite powder were mixed at equal molar amounts as the source materials, and they were placed at the center of a pyramid-like quartz tube. The quartz tube was then placed in a tube furnace, which was later heated to 1100 °C within 90 min. The as-grown product was collected at the wider side of the pyramid-like quartz tube. The morphology and high-resolution images of the sample were observed with scanning electron microscopy (SEM, Hitachi S-5200) and high-resolution transmitted electron microscopy (HRTEM, Phillips FEG-CM 200). The powder was dispersed into ethanol for optical analysis. A TU-1901 UV−vis absorption spectrometer and a PTI−C-700 fluorescence spectrometer were used to obtain its absorption and emission spectra, respectively. A CW He−Cd laser (50 mW, wavelength at 325 nm, IK 3552R-G) was used to measure the photoluminescence of the sample and its stimulated emission.

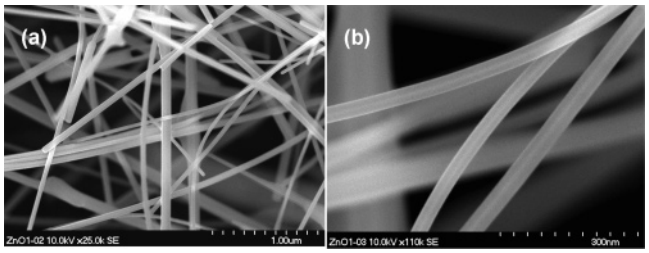

Figure 1. SEM images of the as-synthesized zinc oxide nanowires and nanobelts.

The morphology of zinc nanowires is shown in Figure 1 a and b. Many prismatic rods whose diameters are about 50−150 nm are randomly distributed on the substrate. The sample is pure and clean.

Figure 2a is the absorption spectrum of ZnO nanowires, which shows a sharp excitonic peak at the band edge, and the first peak maximum is about 373 nm. There are several peaks in the range of 250−360 nm, analogous to those for the CdSe and CdS quantum dots. The oscillator strength of the first transition (at 373 nm) at room temperature is rather high, which has rarely been observed.[1−5] The arrowhead in panel a indicates the first transition line of 5 nm zinc oxide nanocrystal at about 360 nm due to the quantum confinement effect. As the particles extend along a line to form a nanowire, the bandedge redshifts to 373 nm as indicated. Moreover the sharp exciton peak at 373 nm indicates a significant exciton confinement, or enhanced exciton binding energy in this structure. High exciton binding energy lead to a longer lifetime of exciton and a long coherence space,

† Micro-Nano Technologies Research Center Hunan University, Changsha.

‡ Beijing National Lab for Condensed Matter Physics, Institute of Physics, CAS, Beijing.

§ School of Materials Science and Engineering, Georgia Institute of Technology, Atlanta, Georgia.

10.1021/jp061357d CCC: $33.50 © 2006 American Chemical Society
Published on Web 06/13/2006

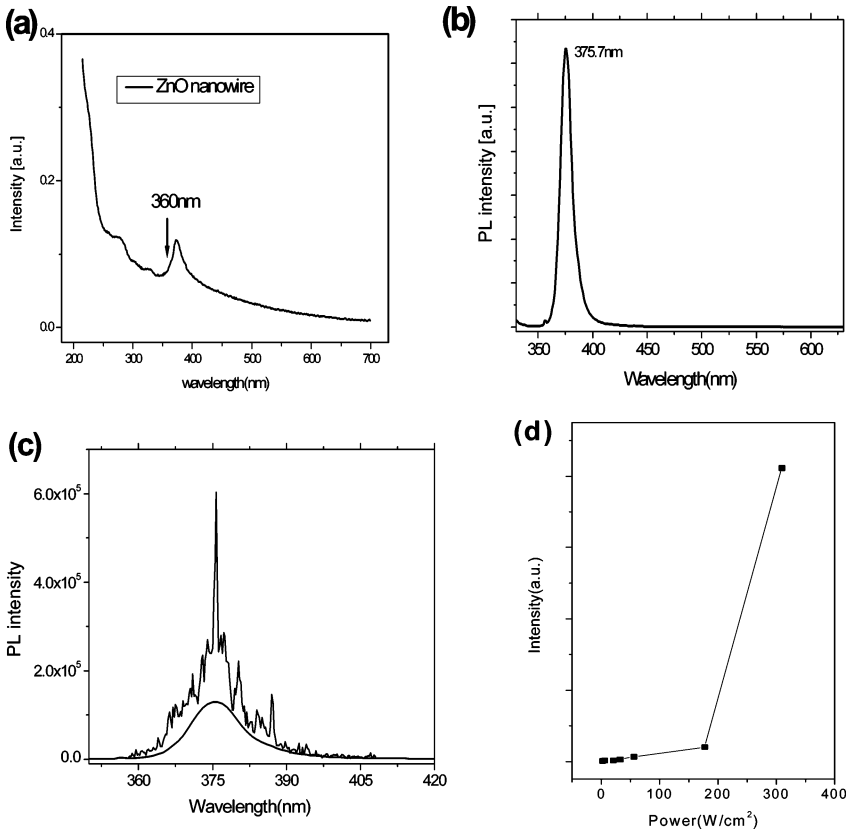

Figure 2. (a) Absorption spectra of ZnO nanobelts; (b) the bandedge luminescence; (c) Stimulated emission spectra; (d) emission intensity vs excitation power.

which can produce exciton−exciton collision and lasing properties at a low concentration.

The photoluminescence spectra and stimulated emission spectra of the nanobelts are shown in Figure 2b,c. The emission maximum is at 375 nm in Figure 2b, which represents a free exciton emission. For the stimulated emission measurement, the optical pump source was the CW He−Cd laser, the output power is, at most, 50 mW, and the output line was focused for adjusting the illumination power with a quartz convex lens. As is well-known, ZnO always produces emissions below the band edge,[12] from the bound exciton, surface states, or impurities, no matter how the sample is prepared. For our sample, no luminescence from surface state or defect state can be detected and only ultraviolet band-edge stimulated emission exists, which can be assigned to the free exciton transition. The photoluminescence fwhm is about 11 nm. The luminescence intensities of ZnO increase when the pumping power was increased. The stimulated emission or the lasing emission spectra are shown in Figure 2c. The background is originated from (1) the spontaneous radiation transition of free excitons and (2) the Brownian motion of the nanowires in solution, *which change the orientation of nanowire temporally*. In Figure 2c, the emission intensity is increased with the increase of power, *as does the optical absorption*. The stimulated emissions were observed at about 200 W/cm^2 with a single mode emission, while multimodes appear at a slightly higher power.

The above phenomena may be assigned to the interplay of the exciton interaction and the cavity effect.[3,5,13] The nanowire can be thought as 1D quantum wire. At first, the spatial confinement in 2D increases the binding energy and lifetime of exciton, which lead to a low threshold power to produce stimulated emission. Second, the photoinduced exciton prefers to align along a line. Each photoinduced exciton can be seen as a QD. Then, if neighboring QDs have the same crystal axis or dipole orientation, they may couple to form a new large-exciton behaving like an aggregate of excitons. Clearly, aggregate itself represents a nonlinear correlation between excitons. In such situations the excitonic coherence may lead to giant oscillator strength with or without polariton,[14,15] which will exhibit giant nonlinear optical responses. If the first transition in a single QD is dominantly radiative, the collective radiative emission will also dominate in the large exciton relaxation at critical excitation. The absorption peak at 373 nm in Figure 2a is evidence of excition effect and could induce the giant oscillator strength of excitons for their high binding energy (over 60 meV absolutely), *as verified by absorption coefficients variation with power*. Third, the multimode is originated from F−P effect of the bound exciton and free exciton emission in a broad range. Clearly the lasing phenomenon in pure ZnO nanowire comes from the exciton−exciton interactions and related giant oscillator strength effect *except that under very high excitation*.

3. Mn(II) Doped ZnO Nanowires

The Mn(II) doped ZnO nanowires were synthesized via a technique similar to that described above. The oxide source material was a mixture of 10% MnO powder and 90% ZnO powder. The detailed preparation process is given in ref 12. The SEM images (Figure 3a) of the ZnO nanowires indicated that the nanowire length was above 10 μm and the average diameter is 500 nm, with a regular hexagonal cross section. HRTEM observation indicated that all nanowires grow along the *c*-axis (Figure 3b). The chemical composition was also checked by energy-dispersive X-ray spectroscopy (EDS) equipped in TEM, shows the presence of Zn and O elements, but the content of Mn is below the detection limit of EDS. By using inductively coupled plasma-mass spectrometry (thermo element $\times$7), 0.6−25 ppm Mn was detected in the sample.

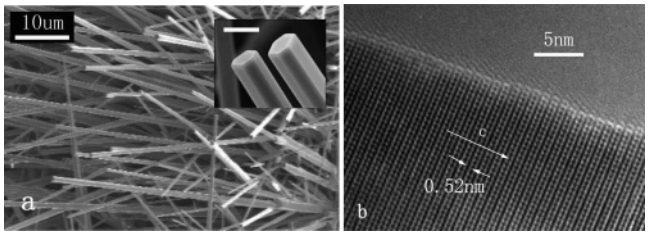

Figure 3. (a) SEM image of the as-grown nanowire array. Inset is a high-resolution SEM image of the nanowires, the scale bar is 500 nm. (b) A high-resolution TEM image of a nanowire, and the arrowhead indicates the growth direction. The scale bar is 5 nm.

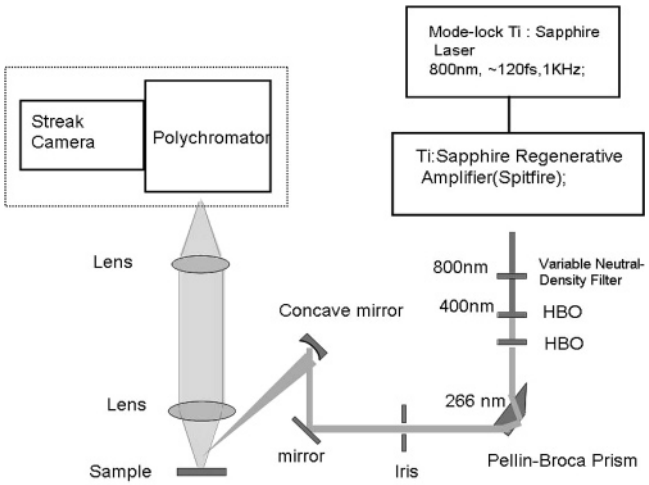

Figure 4. The setup for PL and lasing experiments of the nanowires. 800 nm beam is generated by a regeneratively amplified Ti-sapphire oscillator (120 fs pulse width, 1 kHz). The streak camera system was used to detect the PL and lasing signal generated from nanowires which excited by the 266 nm fs pulse.

The experimental setup for laser excitation and emission probe is show in Figure 4. Photoluminescence (PL) was obtained with excitation of ~fs pulsed UV line at room temperature. The laser excitation source derived from a regenerative amplifier (Spitfire, Spectra Physics), which was seeded by a mode-locked Ti-sapphire laser (Tsunami, Spectra Physics) for delivered laser pulses of 800 nm (~120 fs, 0.7 mJ, 1 kHz). The frequency was doubled by a BBO crystal to generate the second harmonic line at 400 nm. This laser line then passes through another BBO crystal, in which the mixing signal was generated at 266 nm. The highest output energy could be 10.5 μJ/pulse before focus. A variable neutral-density filter was used in front of the first BBO to calibrate the output power. The PL signal was collected by the microscope objectives and then focused into a polychromator. The PL was detected using a photon counting streak camera (Hamamatsu C2909), the time resolution was 20 ps and the spectral resolution of polychromator with 150 lines grating was 0.2 nm.

The photoluminescence spectra of ZnO nanowires under varied excitation powers are shown in Figure 5. In the low pump power region, two PL bands are observed for this low Mn doped nanowires, one from free exciton is marked by arrowhead A and a significant companion-band was marked by arrowhead B. They were located at 3.305 and 3.168 eV, respectively. Their energy width is 137 meV. This energy spread is surprisingly equal to the energy of two-phonon band (the overtone of A1 phonon mode), so the companion-band B should be a polaronic exciton (bound excitons). With the rise in the excitation power, the B band increases with a superlinear rate. In contrast, the free exciton (A) band showed almost no rising with the increase

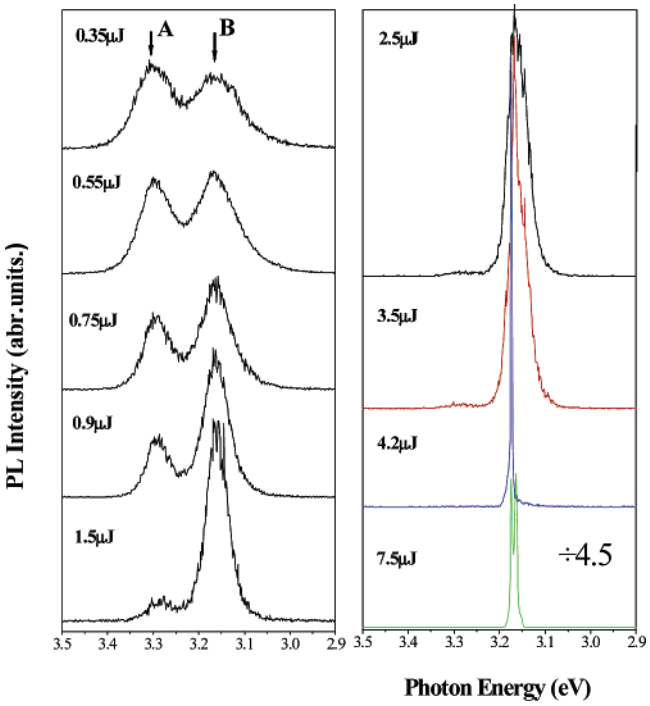

Figure 5. Photoluminescence of ZnO nanowires at various pumping energies.

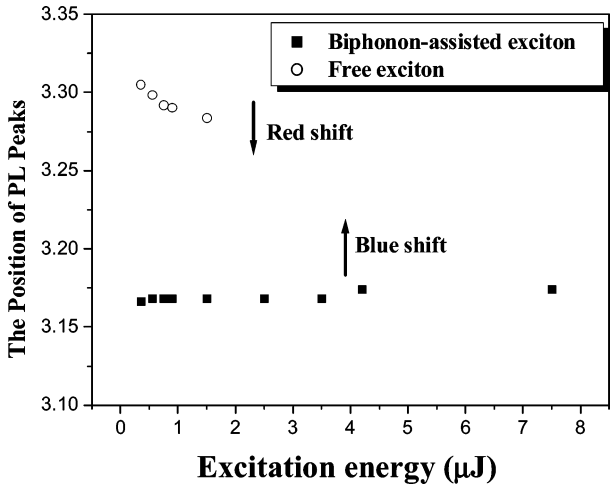

Figure 6. The photoluminescence peak position from free exciton and 2LO phonon-assisted complex, respectively, showing their dependence on the excitation power, whose magnitude corresponding to the exciton density in the nanowires.

in excitation power in the relatively low excitation range. In the slightly high power range, the free exciton band (A) weakens whenever the B band enhances with power. Then the A band diminishes until pump power reaches 2 μJ/pulse. In the even high power range, only the B band was left. When the excitation power reached 3.5 μJ/pulse, the entire PL becomes stimulated emission of B band without any spontaneous radiation background. Its peak position is blue-shifted about 50 cm^{-1} from its original position at low excitation as shown in Figure 6. This shift is likely due to the phase space filling effect of excitons at high excitation[16] that represents exciton population without carrier scattering. This stimulated emission indicates a coherent transition of bipolaronic states. When the excitation energy reached 4.2 μJ, the lasing band became much narrower than the low excitation, a super-narrow line with full-width at half-maximum (fwhm) of 3 meV in the emission spectra was observed. Further increasing of the excitation power to 7.5 μJ

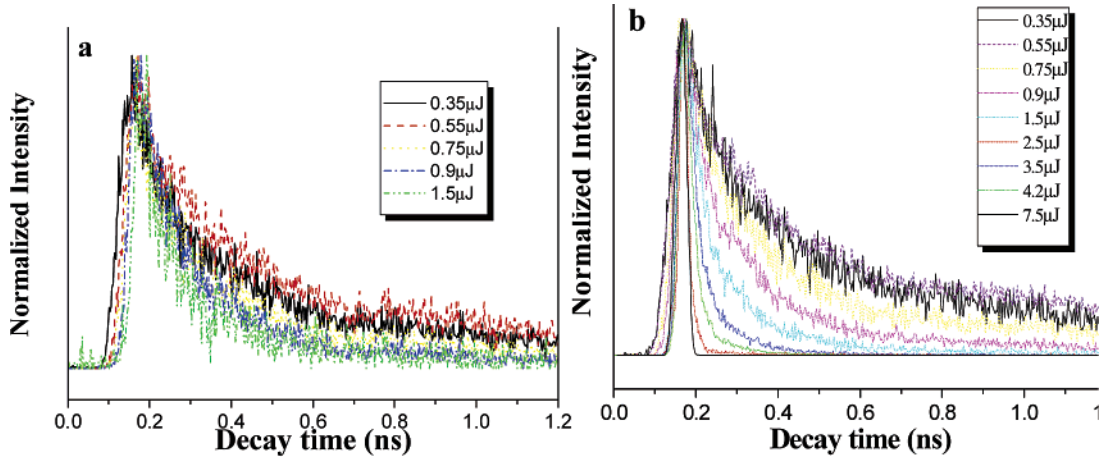

Figure 7. Decay times of photoluminescence with various excitation energy from (a) free exciton and (b) the complex with 2LO phonon, respectively.

finally led to the occurrence of the second peak with an energy width of 10.5 meV in its red-side. The splitting may comes from the dipole−dipole interaction of different coherent states. In this entire process, the fwhm of the A and B bands become narrower with the increase in excitation power, and finally the emission bands converge to a line near the B band. For a higher Mn ion doped nanowire sample (no more than hundreds ppm range), we observed the dominant B band with a very small shoulder of A band at low excitation. The emission behaviors of these samples at high excitation is similar to that of the less doped nanowire sample, and the threshold power to produce stimulated emission is slightly lower than that of the less doped nanowires. For over 200 ppm Mn doped ZnO nanowires, we observed multimode lasing, silimilar to that of Fabry−Pyrot cavity effect by the electron−hole plasma, which will be discussed in the next section. The single mode emission differs from those results of bound excitons in the literature, but much like the BEC [Bose−Eeinstein condensation] of excitons.[17]

Why did the A band disappear in high excitation power and change at varied Mn doping levels? This question is related to the nature of excitons in this system. The large exciton binding energy (60 meV) and strong electron−phonon coupling in ZnO are critical to determining the exciton stability and emission process at room temperature. The free exciton (the A band) should be prevailing due to the high binding energy (60 meV) under low excitations for pure crystal. The B band originated from the significant exciton−phonon coupling, i.e., it is the two A1 phonons coupled exciton (polaronic exciton), which is still movable like free exciton at room temperature. So the latter, the phonon coupled exciton (polaronc) has a higher binding energy, i.e., the sum of 60 meV (free exciton) and 137 meV (two-phonon energy). Hence, the A and B bands in this nanowire could occur simultaneously owing to their high stability in reference to thermal energy (26 meV) at room temperature. The B band appearance depends on the ion doping, which enhances the electron−phonon coupling and also exhibits higher binding energy. In a higher Mn doped nanowire, a dominant B band emission occurs. The emission spectra without the one-phonon sideband indicate a significant nonlinear coupling in this 1d system and 1-phonon transition is not parity allowed.[18] This nonlinear coupling may facilitate the coupling between excitons via phonons with increasing density. When the second exciton occurs to bind with polaronic exciton, the bipolaronic excitons form in a nonlinear coupling and coherent state.

The reduction of free exciton band in Figure 5 means the reduction of its binding energy. The binding energy of free exciton can be decreased (as shown in Figure 6 the redshift of A band) by two causes: (1) pairing or aggregating of neighboring excitons or binding to other elementary excitation, (2) the screening of enhanced Coulomb interactions between free carriers due to the band-gap renormalization, both evidenced by the observation on the red-shift of the A band as shown in Figure 6. For no e−h plasma state is observed, so the factor 1 should be dominant. It is clear that the subsequently excited excitons prefer to bind with the preformed polaronc excitons and populate at the low energy states (the B band), which accounted for the disappearance of the A band at high density. This phenomenon indicates the interactions between these excitons are attraction force, which is easily realized in head to tail dipole connection of excitons in 1d alignment.[19]

There is another reason for the free excitons transferring to two-phonon bound exciton band (the B band). The fs laser could produce coherent excitonic states, which even could stand for very a long range.[20] Multi-phonon coupled free excitons coherently turn into the bipolaronic excitons at a suitable density (here at about 4 μj/cm^2), forming a four-particle state with two phonons and two excitons, like the BCS Cooper pairs in a superconductor, which could overwhelm the repulsion of exciton repulsion for further condensation. Such as the Fermionic atom condensation which happened from the pairing of atoms.

In this experiment, the B band emission showed strong tendency to keep exciton coherence under higher excitation. From 2.5 to 4.2 μJ, the band-like emission turns gradually into a single line emission as a coherent collective radiation, up to 7 μJ. This differs from those lasing from electron−hole plasma (EHP),[21−25] in which spectral broadening and red-shift were generally observed with multimode lasing. In this case, the A and B bands can coexist only at the low excitation for their high stability. Further spectral variations indicate the B band is originated from a more stable state. Figure 7 shows the decay profile of the A and B bands. The different PL decay profiles were related to their different lifetimes and relaxation processes. The free exciton and biphonon bound exciton emission decay shows change when excited with varied powers as showed in Table 1. The ~ps decay time at low excitation corresponds to the free-exciton recombination rates in the bulk. For the high density, the relaxation rate goes faster and faster, for two components, up to the low detection limit. The fast component represents the correlated state due to exciton coupling, and the slow component represents the spontaneous emission of this exciton in situ. This fact clearly shows that there were interactions that led to their collective relaxations (fast component) in the free exciton relaxation except for the inner conversion below the critical density. The B band decay shows

TABLE 1: The Decay Times for the Two Bands under Different Excitation Energies

	decay time of free exciton	decay time of 2LO-assisited excition
0.35μJ	t_1 = 133ps; 67%	t_1 = 155ps; 63%;
	t_2 = 898ps; 33%	t_2 = 1.36ns; 37%
0.75μJ	t_1 = 110ps; 68%	t_1 = 103ps; 66%;
	t_2 = 706ps; 32%	t_2 = 731ps; 33%
1.5μJ	t_1 = 32ps; 67%	t_1 = 31ps; 74%
	t_2 = 192ps; 33%	t_2 = 142ps; 26%
2.5μJ	unable to be detected	t_1 = 26ps; 89%
		t_2 = 108ps; 11%

a similar profile at lower power, but goes faster at higher power. The transfer (inner conversion) rate from A to B, goes faster at higher excitation, and it determines the lifetime variation of the A band. In Table 1, the longer lifetime of the B band proved a higher stability of the B state, the fast increasing and narrowing of the B band indicates a condensate formation, which is like that of the bipolaronic exciton formation (at 4 μj/cm^2 in this case). That is to say, two-phonon bound excitons can form bipolaron with subsequent free exciton. After bipolaron formation the blue shift of B band at 4 μj/cm^2 indicates a small coulomb repulsion due to the bipolaron *interaction in this condensate*. The *initial* driving force, *which is crucial to exciton stability*, is the nonlinear coupling of two-phonons to exciton with a bipolaronic attraction, 1d structure facilitate their attractions. This kind of interaction therein can avoid EHP [e−h plasma] formation. So the above processes seem much like the BCS condensate clearly evidenced by a strong attraction between bound excitons *via biphonon*, the difference is that the BCS pair is composed of an electron and phonon, instead of an exciton and phonon. Besides the coherent behavior, another reason we call it a *condensate* is the *repulsion interaction between final bipolaronic excitons*, this is an important characteristic of a Bose condensate.

It is well-known that the Mn ion doped ZnO takes on the ferromagnetic properties[26,27] of hole doped or of Mn ion partially oxidized above a critical concentration. The PL emission of bound exciton by Mn doped ZnO was reported to be around 370−420 nm.[28,29] These earlier reports indicated that the doping impurities might lead to significant change in the electronic structure and properties of ZnO.[27,30−32] Therefore, it could be inferred that there is a possible phase in lower doped ZnO, in which the phonon-coupled exciton should be a dominant excitation related to the multi-phonon mode involving Mn ions. Ferromagnetic coupling could not be avoided, and the coherent excitons might also account for the interaction between magnetic polaronic excitons. Ferromagnetic coupling between excitons were certainly to be a positive driving force to put these excitons together to condensate.[26,27] Therefore, the photoinduced magnetic polaronic excitons, generated by an fs laser pulse, could be a significant candidate for generating the long lifetime states to realize BEC in a real confined space.

The single mode laser emission without electron−hole plasma (EHP) at high excitation density described above occurs by using fs laser pulse to pump. When the fs laser pulse excited the nanowires in ~120 fs, at least ~10^{18} excitons could be created, according to the photon scaling in the illuminated area. For nanowires with 10 μm length and 500 nm thickness, it can afford 10^6 excitons. So the fs laser pulse can produce enough excitons in one pulse if other losses are subtracted. The biexciton cannot be a channel for this decay, because (1) there is no biexciton identification in ZnO crystal, and (2) no emission band related to biexciton occurs together with a broad free exciton band. The general co-occurrence of single-exciton emission band with

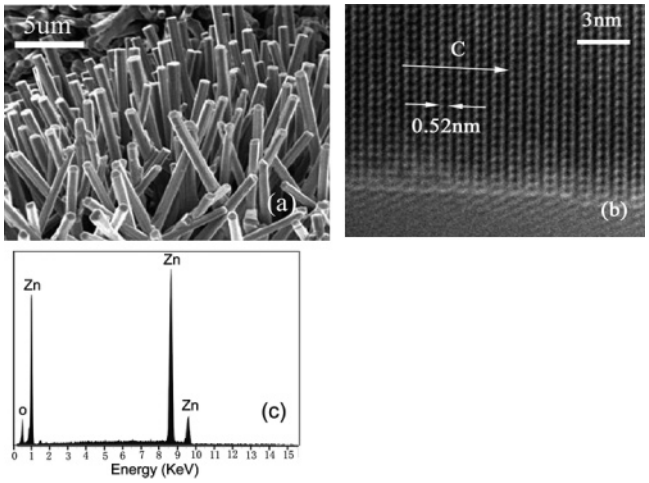

Figure 8. (a) SEM of as-grown nanowire array; (b) A high-resolution TEM image of a nanowire, and the arrowhead marks the growth direction; (c) The energy dispersive spectroscopy (EDS) taken from a ZnO nanowire.

biexciton band at high density was not observed in our experiments. The single mode lasing, as in previous literature, which often shows up over a broad and weak spontaneous emission band as in Figure 2c, is also not found in this case. We cannot detect the exact dynamic times for exciton generation, condensates formation and relaxation directly due to the limitations of the detector resolution. This condensate might not possess a long lifetime due to its transition rule and dynamic nature. Leung et al.[32] studied the time-resolved stimulated emission and observed the formation time at about 5 ps for the free exciton in ZnO, this value may be comparable to or a little shorter than the exciton condensate. Another consideration for the change of PL bands due to exciton−polariton is also not plausible for the pump condition and no Rabi profile due to the coupling photon and exciton. Therefore, this single mode is a dynamic condensate in 1d nanowire.

There should be a critical size of nanowire to realize the phonon-assisted BEC. This occurs at the quasi-one-dimensional structure of length close to several micrometers, which cannot be considered as absolute 1D nanostructures because the width of wire could contain several tens excitons across the cross-section. This 1D structure only supplies a confined space for excitons to reach the critical concentration, and the mobile excitons only move along the 1D axis coherently. The nanowire, therefore, could limit the expansion of excitons in two directions and facilitate the combination of the 2LO phonon mode[33] with excitons[18] and also the condensation.

The fs pulse is another advantage in producing coherent excitons and realizing temporal Bose condensation. Anexcitation of 120 fs and thereafter relaxation time, not many excitonic carriers were lost due to the motion expansion or collision and other nonradiative pathways before condensation. A great number of excitons can be created in a short time to reach the threshold density of Bose condensation. The other advantage was that fs pulses almost did not destroy the samples because, in its short interaction time, the lattice temperature would not increase significantly. The high lattice temperature would lead to the exciton dissociation.

4. Heavily Mn(II) Doped ZnO Nanowires

The sample was obtained by similar technique, the reaction proceeds with 20% MnO + 80% ZnO for half an hour at 1000 °C. The average length of the nanowire is 10 μm, and diameters

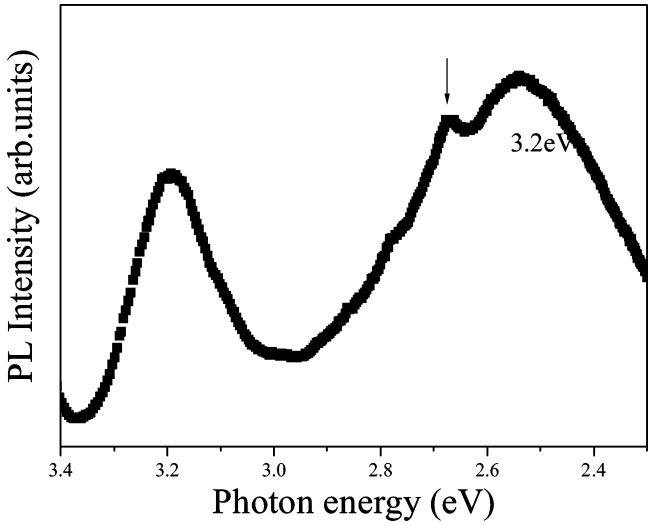

Figure 9. The PL of ZnO nanowire excited by Xe lamp.

range between 300 and 700 nm. Figure 8a shows the SEM images of ZnO nanowires on ZnO substrate. Figure 8b shows the HRTEM images of the edge of a single nanowire, which indicates that all nanowires grow along the [0001] with good crystallinity (the *c*-axis growth direction marked by the arrow). Only Zn and O were detected by EDS in the sample as shown in Figure 1c. The Mn (II) concentration is about 0.002−0.00028 atomic percent by ICP technique.

Figure 9 shows the PL of a ZnO nanowire excited with a Xe lamp at room temperature. The Xe lamp was used for low excitation to compare with the high excitation of a nanosecond or fs laser. We can see two emission bands, as shown in Figure 2, one corresponds to the green luminescence band from the trapped states,[34] and the other corresponds to the near-band-edge emission, which is at 3.2 eV with a broad fwhm of 164 meV. This band will broaden for the heavily Mn dopped sample, and it is the convolution of the optical transition of free excitons, especially the 1LO-assisted excitons and 2LO-assisted excitons. This fwhm at low excitation is broader than that realized with fs laser excitation. The sharp peak at 2.72 eV (465 nm) is the strongest scattering band from the Xe lamp. Under ns laser excitation, we found that the two emissions, UV band and green band, varied depending on the pump fluence in the limited space.

For such nanowires, the waveguide behaviors exist in its emission.[10,23] The PL from UV band and green band all show nonlinear behaviors at high excitation, while linear optical responses are produced in low excitation. Figure 10 shows the evolution of PL with increasing pump fluence of fs pulse around the threshold pump fluence, and the experimental setup is schematically shown in the inset at left. The threshold at around 26 μJ/cm^2 was obtained, as shown in the inset at right in Figure 10. Over the threshold, we see a rapid growth of the peak at 3.19 eV at the blue side of the spontaneous radiation band, with the appearance of a super-narrow line of fwhm 12 meV. The luminescence output is in proportion to the square of the excitation energy (26−56 μJ/cm^2), that is $I_{\text{lumi}} \propto I_{\text{exc}}^2$. Over 56 μJ/cm^2 the emission intensity tends to be saturated with multimode lasing, which is similar to the EHP phenomenon observed by Yang et al.[23] The value for saturation reduces with rising Mn(II) doping. For the green band emission, we can occasionally see a linear increase with excitation power, sometimes an early saturation below the UV band needed exctitation power can be observed. Stimulated emission can only be observed for the UV band.

The dynamics of the two kinds of PL bands with the pump power were shown in Figure 11. The rise time (∼1.5 ns) and the decay time (longer than 10 ns) corresponding to green emission with 21 μJ/cm^2 pump power were obtained, as shown in Figure 11 a. A much shorter decay time (∼110 and 32 ps corresponding to pump fluence 21 μJ/cm^2 and 38.5 μJ/cm^2, respectively) for UV band were observed in Figure 11b. The rise time in Figure 11b cannot be resolved well due to the limited time resolution of the streak camera. The rise time (1−2 ps) for exciton−exciton recombination and EHP was mentioned in the previously reported results.[25,32,35] The rise time correspond-

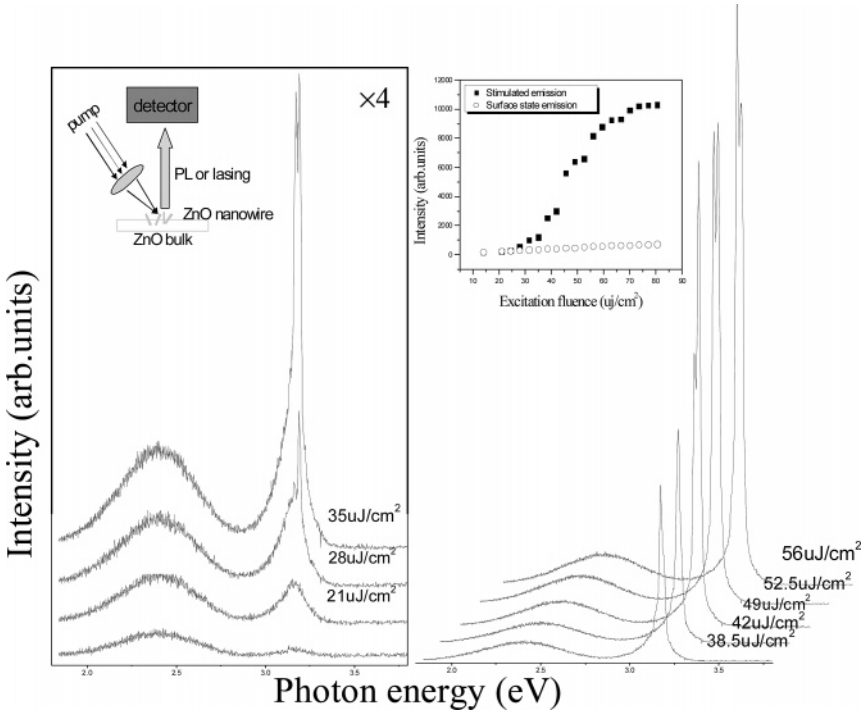

Figure 10. The PL dependence of the pump fluence from ZnO nanowires. The setup of PL is schematically shown in the inset at left; the inset at right side shows the UV emissions as a function of the pump fluence compared with the green emission.

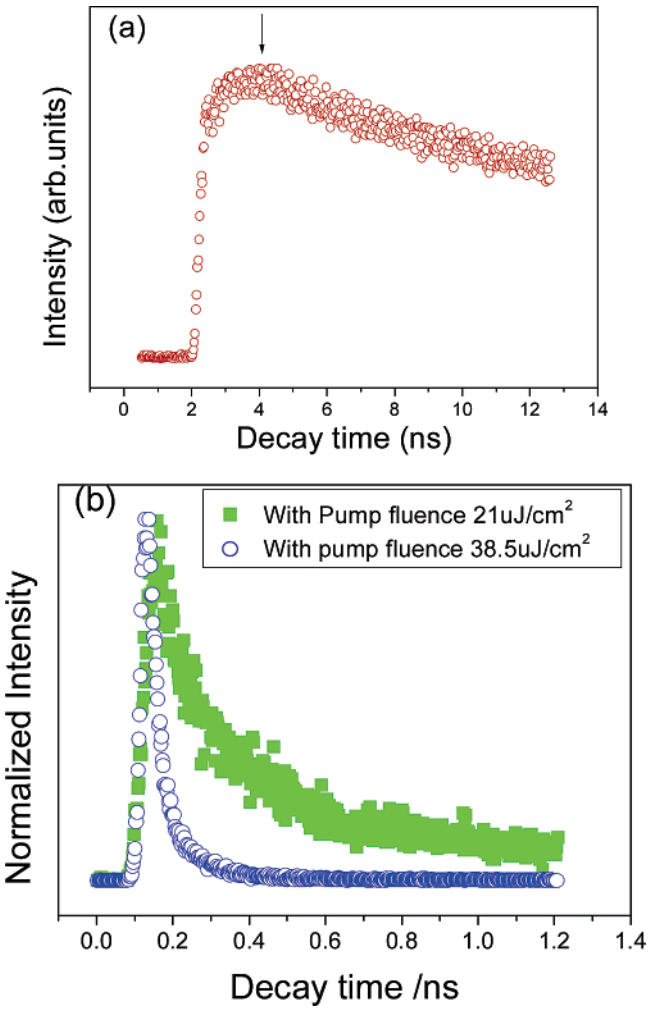

Figure 11. (a) The decay time of the green emission with 21 μJ/cm^2 pump fluence and (b) UV emission with 21 μJ/cm^2 (square) and 38.5 μJ/cm^2 (circle) in ZnO nanowires, respectively.

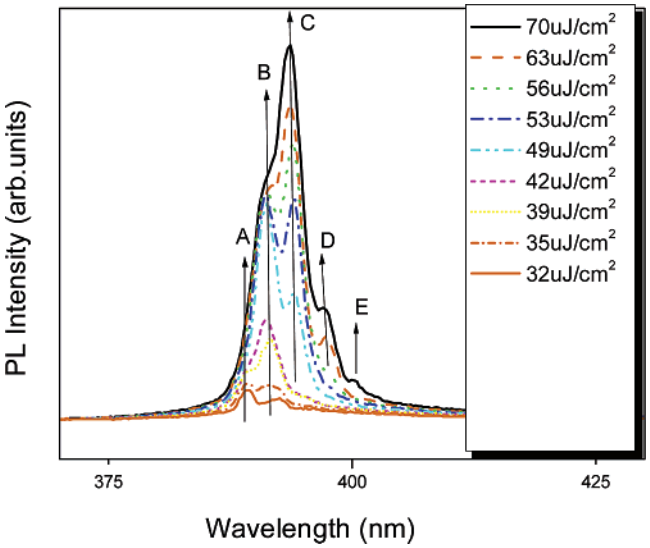

Figure 12. The detailed variation of lasing multi-modes with the pump fluence increase in ZnO nanowires. The direction of arrows shows the increase of pump fluence; the mode marked by arrowhead B appears latter than A with pump fluence increase, and further, the modes marked by arrowheads C, D, and E appear.

ing to the green emission marked by the arrowhead in Figure 11a is far longer than that of the UV emission. This demonstrates that the defect and surface states population is too slow to block the UV stimulated emission. That is to say, the UV emission can become the dominant decay pathway at high excitation. For even higher excitation, the exciton−exciton collision and exciton−phonon coupling enhance to dissociate the exciton, therein many free carriers led to e−h plasma formation, which accompany the band red shift and broad band emission. The emission can be saturated by the coulomb repulsion and auger process in multi-carrier system.

Another interesting thing is the stimulated emission band is located at 382−390 nm in the intermediate excitation range, which is different from that of the low-Mn nanowire. That means the bound exciton by impurity plays a dominant role in the emission spectra. With the rising pump power, the narrowing in spontaneous emission band was accompanied by the appearance of lasing modes, as shown in Figure 10. Because the spontaneous emission and stimulated emission occurs with much spectral overlap, the lasing modes are behaved by the superposition with amplified spontaneous emission (ASE). At the fluence just above the threshold (2.6 μJ/cm^2), we see two supernarrow peaks appearing at the blueside of spontaneous radiation band, with the one located on the blue side being stronger than the other on the red side. These should be all the longitude cavity modes along the *c* axis of the ZnO nanowires. The first mode corresponds to the optical gain maximum. As the pump power increased further, the second longitudinal mode develops on the low-energy side when the gain corresponding to the mode overcomes the loss during propagation along the *c* axis of the ZnO nanowire. With a further increase of pump power, more and more modes appear with even higher carrier densities within the nanowires. According to the condition of the Febry−Perot laser cavity, the two neighboring modes will be satisfied with the following relationship (the variation of the refractive index being ignored):

$$\Delta\lambda = \frac{\lambda_1\lambda_2}{2Ln}$$

Here, L is the length of the nanowire in which the lasing multimodes were generated, and n is the refractive index at λ_1 or λ_2 (the wavelength of one of the modes) of ZnO. The refractive index is around 2.45 for the wavelength at 390 nm. The length of the nanowire was obtained from the formula of longitude mode space along the *c* axis in the nanowire. The peaks marked by the arrowheads are at 391 and 393.7 nm, 397 and 400 nm, respectively, as shown in Figure 12. The length of the corresponding nanowire, 10.55 μm, was deduced. After that, the length is used to test the validity of different wavelengths; each wavelength of the multipeaks in the PL spectra agrees well with individual values calculated by the by the formula. Coexistence of multi-cavity-mode demonstrates the high quality resonant cavity effect in this nanowire, especially for the plasma emission.

Figure 12 shows the changes of different modes in response to different high excitation. We can see that the strongest mode moves from 391 to 393.7 nm, then to 397 nm, and even reaches 400 nm. With the pump power increase, the carrier density and carrier interactions become stronger and stronger and then the effect of band gap renormalization appears due to coulomb repulsion and Auger processes. The red shift of ASE position reflects this process. Therefore, many lasing modes appear at the same time in the ASE emission packet demonstrates the electron hole plasma processes and good quality of the end facet of the nanowire.

In this heavily Mn doped ZnO nanowire, in contrast to low Mn doped nanowire and pure nanowire, free exciton emission cannot be observed due to relatively strong scattering of impurity and phonon. The bandedge emission was dominated by the bound exciton, which bring in by doping the nanowire. This result indicates that free carriers still are not the dominant excitation in this nanowire, for their EHP behaviors are only induced by much higher excitation. Clearly, the interactions between bound excitons dominated the radiative process at the early stage of laser pump, although they are a little complicated for the participation of free carriers and impurity, which were also the origin of exciton dissociation. Rising pump fluence can induce stimulated emission due to exciton−exciton interaction in the intermediate fluence range, in which the emission intensity increases swiftly. The results reflect the giant oscillator strength effect and cooperative radiation of localized excitons.[14,15] Further rising power turns the nanowire into an EHP-dominated stimulated emission in the high power range, in which coulomb repulsion and Auger process is significant, to lead to clear band broadening, saturation, and band redshift[16] combined with the multimode lasing. The laser threshold for EHP formation can be found to reduce with increasing Mn concentration. It should be indicated that the EHP formation can damage the sample if it sheds the fs pulse beam of high power for up to several tens of minutes.

From the above discussion, the binding energy of exciton in nanowire is lifted due to the confinement, which dominates the emission process of the nanowire. This concept works for free exciton, polaronic exciton, and bound exciton. These three states of excitons can be tuned in order by doping the Mn ions with varied amounts at room temperature. Hence doping can change the exciton type and related interactions. Although there is no $Mn2^{+}$, polaronic excitons can bind with each other to form bipolaronic excitons in 1d nanostructure and produce the highest binding energy. So excitonic behaviors in 1d nanostructure still determine the optical properties of nanowires at room temperature, in which the giant oscillator strength effect takes effect for varied prevailing excitations in differing doped nanowires; bipolaronic exciton may produce a macroscopic quantum state and clean coherent emission. They all show prominent lasing emission after photoexcitation, but multimode emission is dominant in free exciton and bound exciton systems under very high excitation for relatively low stability. The next step is to find a way to inject electrons by electrical techniques.

It is surprising that there is a new phase of bipolaronic exciton condensate to contribute to the lasing phenomenon in nanowires. In this nanowire, Mn(II) is slightly doped in and plays a role in enhancing electron−phonon coupling. So the polaronic exciton, with larger binding energy, is photoinduced to concur *and bind* with another free exciton. The 1d aligning of exciton favors attraction coupling, so aggregated polaronic excitons gradually become the only state at high excitation. Moreover, the largest LO phonon in the *c* axis contributed to this condensate formation. This finding may be a chance to realize the BEC of excitons in semiconductor nanostructures.

Conclusions

In this paper we reported three types of lasing mechanism in ZnO nanowire, pure, lightly doped, and heavily doped. Except the exciton−exciton interaction, we found a new phase in ZnO nanowire for the lasing, which is bipolaronc exciton condensate, a typical 1D phenomenon in semiconductor nanostructures. The different lasing mechanisms are determined by the interplay of the exciton binding energy, doping, exciton−phonon coupling, and F−P effect. The doping can change the exciton−phonon coupling significantly, which therefore, tunes the binding energy of excitons, bound exciton formation, and exciton dissociation processes. These results may find important application in future ZnO photonic devices.

Acknowledgment. We are grateful for the financial support to NSFC of China (term no. 20173073), National 973 Project (2002CB713802), 985 project of HNU. All authors are grateful for the experimental supplying of State Key Laboratory for Structrural Chemistry of Unstable and Stable Species, Institute of Chemistry, Chinese Academy of Science, China.

References and Notes

(1) Zamfirescu, Marian; Kavokin, Alexey; Gil, Bernard; Malpuech, Guillaume; Kaliteevski, Mikhail *Phys. Rev. B* **2002**, *65*, 161205(R).

(2) Bagnall, D. M.; Chen, Y. F.; Zhu, Z.; Yao, T.; Shen, M. Y.; Goto, T. *Appl. Phys. Lett.* **1998**, *73*, 1038.

(3) Bagnall, D. M.; Chen, Y. F.; Zhu, Z.; Yao, T.; Koyama, S.; Shen, M. Y.; Goto T. *Appl. Phys. Lett.* **1997**, *70*, 2230.

(4) Cao, H.; Zhao, Y. G.; Ho, S. T.; Seelig, E. W.; Wang Q. H.; Chang R. P. H. *Phys. Rev. Lett.* **1999**, *82*, 2278.

(5) Kong, Y. C.; Yu, D. P.; Zhang, B.; Fang, W.; Feng, S. Q. *Appl. Phys. Lett.* **2001**, *78*, 407.

(6) Havam, J. M. *Solid State Commun.* **1978**, *26*, 987.

(7) Havam, J. M. *Solid State Commun.* **1973**, *12*, 95.

(8) Tang, Z. K.; Wong, G. K. L.; Yu, P.; Kawasaki, M.; Ohtomo, A.; Koinuma, H.; Segawa Y. *Appl. Phys. Lett.* **1998**, *72*, 3270.

(9) Huang, Michael H.; Mao, Samuel; Feick, Henning; Yan, Haoquan; Wu, Yiying; Kind, Hannes; Weber, Eicke; Russo, Richard; Yang, Peidong *Science* **2001**, *292*, 1897.

(10) Cao, Li; Liu, D.; Zhu, X.; Zou, B. S. *PLDS* **2006,** in press.

(11) Pan, Zheng Wei; Dai, Zu Rong; Wang, Zhong Lin *Science* **2001**, *291*, 1947.

(12) Monticone, S.; Tufeu, R.; Kanaey, A. V. *J. Phys. Chem. B* **1998**, *102*, 2854.

(13) Wiersma, D. *Nature* **2000**, *406*, 132.

(14) Takagahara, T.; Hanamura, E. *Phys. Rev. Lett.* **1986**, *56*, 2533.

(15) Hanamura, E. *Phys. Rev. B* **1988**, *37*, 1273.

(16) Schmitt-Rink, S.; Chemla, D. S.; Miller, D. A. B. Linear and nonlinear optical properties of semiconductor quantum wells. *Adv. Phys.* **1989**, *38*, 89−188.

(17) *Bose-Einstein Condensation;* Griffin, A., Snoke, D. W., Stringari, S., Eds.; Cambridge University Press: New York, 1995; pp 330, 507, 524.

(18) Rashba, E. I.; Sturge, M. D. *Excitons;* North-Holland Publishing Company: Amsterdam, New York, 1982; p 178.

(19) Cao, L.; Miao, Y. M.; Zhang, Z. B.; Xie, S. S.; Yang, G. Z.; Zou, B. S. Exciton interactions in CdS nanocrystal aggregates in reverse micelle, *J. Chem. Phys.* **2005**, *123*, 024702.

(20) Awschalom, D. D.; Kikkawa, J. M. Electron spin and optical coherence in semiconductors. *Phys. Today* **1999**, *52*, 33−38.

(21) Tang, Z. K.; Wong, G. K. L.; Yu, P. Room-temperature ultraviolet laser emission from self-assembled ZnO microcrystallite thin films. *Appl. Phys. Lett.* **1998**, *72*, 3270.

(22) Klingshirn, C. *Optical Properties of Semiconductors;* Springer: New York, 1995; p 306.

(23) Johnson, J. C.; Yan, H. Q.; Yang, P. D. Optical cavity effects in ZnO nanowire lasers and waveguides. *J. Phys. Chem. B* **2003**, *107*, 8816−8828.

(24) Johnson, J. C.; Knutsen, K. P.; Yang, P. D. Ultrafast carrier dynamics in single ZnO nanowire and nanoribbon lasers. *Nano. Lett.* **2004**, *4*, 197−204.

(25) Klingshirn, C. Properities of the electron−hole plasma in II−VI semiconductors. *J. Cryst. Growth.* **1992**, *117*, 753−757.

(26) Dietl, T.; Ohno, H.; Matsukura, F. J.; Cibert; Ferrand, D. Zener model description of ferromagnetism in zinc blende magnetic semiconductors. *Science* **2000**, *287*, 1019−1022.

(27) Sharma, P.; Gupta, A.; Rao, K. V.; Owens, F. J.; Sharma, R.; Ahuja, J. M.; Guillen, Osorio; Johansson, B.; Gehring, G. A. Ferromagnetism above room temperature in bulk and transparent thin films of Mn-doped ZnO, *Nat. Mater.* **2003**, *2*, 673.

(28) Wu, J. Z.; Yoo, Y. Z.; Sekiguchi, T.; Chikyow, T. Blue and ultraviolet cathodoluminescence from Mn-doped epitaxial ZnO thin films. *Appl. Phys. Lett.* **2003**, *83*, 39−41.

(29) Norberg, N. S.; Kittilstved, K. R.; Amonette, J. E. Synthesis of colloidal Mn^{2+}: ZnO quantum dots and high-T_c ferromagnetic nanocrystalline thin films. *J. Am. Chem. Soc.* **2004**, *126*, 9387−9398.

(30) Furdya, J. K. Diluted magnetic semiconductors. *J. Appl. Phys.* **1988**, *64*, R29−R64.

(31) Takahashi, Masao Optical band edge of diluted magnetic semiconductors. *Phys. Rev. B* **2004**, *70*, 035207.

(32) Mizokawa, T.; Nambu, T.; Fujimori, A. Electronic structure of the oxide-diluted magnetic semiconductor $Zn_{1-x}Mn_xO$. *Phys. Rev. B* **2002**, *65*, 085209.

(33) Leung, Y. H.; Kwok, W. M.; Phillips, D. L. Time-resolved study of stimulated emission in ZnO tetrapod nanowires. *Nanotechnology* **2005**, *16*, 579−582.

(34) Klochikhin, A. A.; Permogorov, S. A.; Reznitskii, A. N. Multiphonon processes in resonant scattering and exciton luminescence of crystals. *Soviet Physic -JETP* **1976**, *71*, 2230−51.

(35) Vanheusden, K.; Warren, W. L.; Seager, C. H.; Tallant, D. R.; Voigt, J. A. *J. Appl. Phys.* **1996**, *79*, 7983.

(36) Yamamoto, A.; Kido, T.; Goto, T.; Chen, Y.; Yao, T.; Kasuya, A. *J. Cryst. Growth*. **2002**, *214/215*, 308.